Research Article

BIOMEDICAL Journal of Scientific & Technical Research

ISSN: 2574 -1241

DOI: 10.26717/BJSTR.2023.49.007795

Development of Methylcellulose/ Polyvinylpyrrolidone Nanocomposites Enriched with Biogenic Zinc Oxide Nanoparticles for Wound Healing Applications

Md. Monirul Islam[1], Firoz Ahmed[1,2] and Md. Ibrahim H. Mondal[1]*

[1]*Polymer and Textile Research Lab, Department of Applied Chemistry and Chemical Engineering, Rajshahi University, Bangladesh*

[2]*BCSIR Laboratories Rajshahi, Bangladesh Council of Scientific and Industrial Research, Bangladesh*

***Corresponding author:** Md. Ibrahim H Mondal, Polymer and Textile Research Lab, Department of Applied Chemistry and Chemical Engineering, Rajshahi University, Rajshahi-6205, Bangladesh

ARTICLE INFO

Received: February 16, 2023

Published: March 23, 2023

Citation: Md. Monirul Islam, Firoz Ahmed and Md. Ibrahim H. Mondal. Development of Methylcellulose/ Polyvinylpyrrolidone Nanocomposites Enriched with Biogenic Zinc Oxide Nanoparticles for Wound Healing Applications. Biomed J Sci & Tech Res 49(3)-2023. BJSTR. MS.ID.007795.

ABSTRACT

Due to their enhanced antibacterial activity and minimal cytotoxicity, nanocomposite hydrogels have been considered attractive materials for biomedical applications. Maleic acid was used as a crosslinker in the development of methylcellulose/PVP/ZnO nanocomposite hydrogels. FESEM, FTIR, EDX, hemolytic and antioxidant tests were carried out to evaluate the prepared nanocomposites. FESEM and EDX measurements confirmed the presence of ZnO nanoparticles in the polymer matrix. The DLS revealed testing that the particle's maximum diameter is 50.7 nm, confirming the particle size and stability of the biogenic ZnO NPs. ZnO NPs incorporated nanocomposites exhibited excellent biodegradability and enhanced antioxidant activity. MC/PVP/ZnO nanocomposites exhibited a significant zone of inhibition against *E. coli* and *S. aureus* bacteria. The results showed that the prepared nanocomposites have high porosity (>80%), swelling properties, and antioxidant activity (>35%). The hemolytic activity test demonstrates that the developed nanocomposites are nontoxic. These findings significantly support the use of these innovative MC/PVP/ZnO bio-nanocomposite dressings for wound healing applications.

Keywords: Nanocomposite; Methylcellulose; Zinc Oxide Nanoparticles; Wound Healing

Introduction

Chronic wounds are still incredibly difficult to treat in biomedical fields due to their protracted healing times. Bacterial infections, underlying medical disorders (such as diabetes and cancer), malnutrition, obesity, and smoking are a few of the causes of chronic wounds [1]. Hydrogels are 3D polymeric networks that can absorb water or biological fluids and can be chemically or physically cross-linked [2-4]. Hydrogels have recently gained a lot of interest for their use in tissue engineering, drug delivery, self-healing, and biosensors [5]. Methylcellulose (MC) is hydrophilic, which allows it to absorb wound exudate and keep the wound moistened [6]. PVP is a non-toxic, water-soluble, film-forming, and non-hazardous polymer [7]. The US Food and Drug Administration has recognized it as a safe and secure polymer for conducting biological experiments in the pharmaceutical and biomedical fields [8]. PVP wound dressings are developed by crosslinking PVP with PEG and agar and sterilizing them [9]. Along with hydroxyethylcellulose, CMC in its sodium salt form (Na-CMC) was exploited (HEC). Due to its superior mechanical properties, swelling ability, inexpensive cost, and greater number of constituents than pure CMC hydrogels, PVP/CMC blend hydrogel has a significant potential for application as a wound dressing [10,11]. PVP/CMC and PVP/CMC/BA hydrogels might work well for treating and healing wounds [12,13].

Maleic acid (MA) is a biodegradable and biocompatible crosslinker that can be used to create new functional biomaterials [14]. The methylcellulose/ Hyaluronic/ AgNPs hydrogels showed good antibacterial activity as wound healing material [15]. Antibacterial hydrogel films are required to regulate and sustain drug

release in wounds. Cellulose derivatives loaded with metal and metal oxide nanoparticles are antibacterial and mechanically strong. The prepared nanocomposites were effective against both *S. aureus* and *E. coli* bacteria [16]. Zinc oxide (ZnO) nanoparticles are exploited in cosmetics and food packaging because of their natural antibacterial properties. The key advantages of adopting ZnO nanoparticles (ZnO NPs) over Ag nanoparticles were their low cost and colorlessness [17,18]. In wounds, zinc oxide nanoparticles inhibit *S. aureus* and *E. coli* germs. By boosting cellular immunological activity, hydrogels create a moist and hydrated environment for wound healing [19]. Infection of the wound can result in effusion, delayed healing, and abnormal collagen deposition. *E. coli* and *S. aureus* bacteria are common pathogens. These bacteria form enormous colonies within the body [20]. Zinc oxide nanoparticles improve wound healing. Wound healing using zinc oxide nanoparticles ZnO NPs is both cheap and safe [16].

Existing wound dressings have issues such as a lack of porosity, less flexibility, a tendency to stick to the wound surface, and a slower healing process (skin migration, connective tissue synthesis, and blood vessel formation); a poor ability to kill bacteria, difficulty in removing the wound dressing after healing, and the ability to cause allergic reactions. By combining biopolymers, synthetic polymers, and antibacterial nanoparticles to create hybrid-based wound dressings with improved properties, such as providing a moist environment to the wound bed, absorbing wound exudates due to its porous network, promoting good gaseous exchange useful in inhibiting bacterial growth, inducing epithelization and cell migration, and supporting tissue regeneration, they are useful for wound healing applications. To our knowledge, the formation and characterization of MC/PVP/ZnO nanocomposites have not yet been studied. Therefore, the aim of this research is to develop the biogenic ZnO NPs incorporated MC/PVP Bio-nanocomposites for wound healing applications.

Experimental

Materials

Methylcellulose (MC) was purchased from HiMedia, India. PVP, maleic acid, and zinc acetate were purchased from SRL, India, and DPPH from Sigma Aldrich, USA.

Biosynthesis of ZnO Nanoparticles

50 grams of neem leaves were collected from the Rajshahi University campus and rinsed with distilled water. The neem leaves were boiled in 200 ml of distilled water for 20 minutes at 65°C. After being agitated in a magnetic stirrer until the colour changed from orange to brown, the aqueous extract was filtered. To prepare ZnO nanoparticles, 50 mL of extract was mixed with 50 mL of zinc acetate. The solution was thoroughly agitated with a stirrer, and a white precipitate was obtained by adding 10 ml of 0.5 M NaOH while maintaining pH 7.0. After centrifugation, the ppt was dried at 65°C in an oven and was calcined in a muffle furnace for 2 hours at 450°C [21,22]. ZnO nanoparticles formation reaction is as follows-

$$Zn\ (CH_3COO)_2.2H_20\ +2NaOH\ =\ 2CH_3COONa\ +ZnO\ +H_20$$

Preparation of MC/PVP/ZnO Nanocomposites

The hydrogel films were prepared using the solution casting method. Firstly, two solutions of 5% (w/v) MC and 5% (w/v) PVP were prepared separately. The solutions were then blended maintaining an 80:20 v/v ratio, and 10% (based on the total polymer matrix) maleic acid was added. The mixture was then heated for 70 minutes at 85 °C with gentle stirring. Using the same method, composites were made by gradually adding (1 mg/ml in water) suspensions of varying concentrations of ZnO NPs (2, 4, and 6 %)) to the MC/PVP solution while stirring. Then, at 25°C, it was sonicated for 10 minutes. The homogenous MC/PVP/ZnO suspensions were put into a transparent petri dish and allowed to evaporate for 72 hours at room temperature. Then transferred it to the Freeze drier for drying [14]. The reaction mechanism of this preparation is presented in Figure 1.

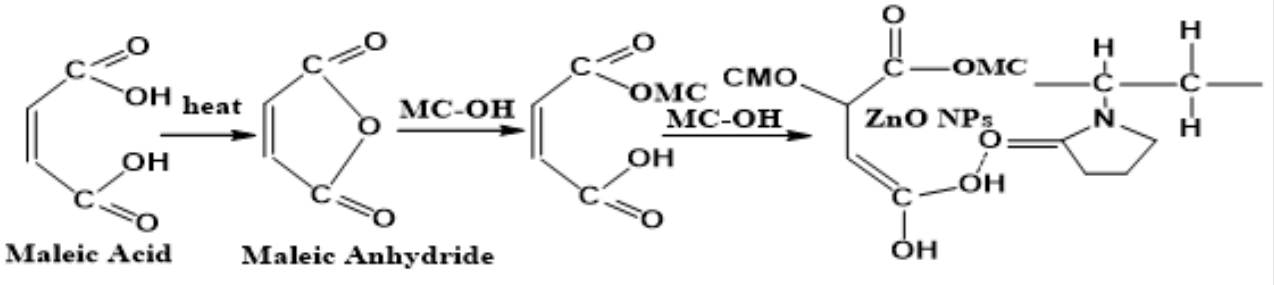

Figure 1: Reaction mechanism for the preparation of MC/PVP/ZnO bio-nanocomposite.

Gel Content

The gel fraction of hydrogels was determined by immersing the sample in distilled water at room temperature and measuring the sample's insoluble portion.

$$Gel\ Fraction, \% = \frac{W_d}{W_i} \times 100$$

Where, W_d is the weight of the dried hydrogel after extraction, and W_i is the initial weight of the dried hydrogel [23].

Swelling Behaviour

A dried sample (1cm × 1cm) was immersed in water at 25°C and withdrawn at predefined time intervals. Surface water is removed using filter paper. Swollen hydrogels were weighed, and the percentage of water uptake capacity was measured by the equation below:

$$S, \% = \frac{M_s - M_d}{M_d} \times 100$$

where S is the equilibrium water absorbency (%); M_s and M_d are the weight of swollen hydrogel (g) at the time (t), and dry hydrogel (g), respectively [24]. Moreover, the capability to absorb water in simulated gastric fluid (SGF) at pH 1.2 and phosphate buffer solution (PBS) at pH 7.4 was assessed. The data represented the average results of three separate tests [25].

Water Vapour Transmission Rate (WVTR)

The European Pharmacopoeia (EP) standard was employed in the determination of the Water Vapour Transmission Rate (WVTR). A 35 mm inner diameter container with 25 ml of distilled water was filled with hydrogel film samples (3 mm thick), which were then cut into circular pieces and taped to the mouth. After that, the bottles were maintained in an oven with a 35°C temperature and a 35% relative humidity level. The WVTR (g/m^2-day) calculation formula is provided below.

$$Water\ Vapour\ Transmission\ Rate = \frac{W_i - W_f}{A} \times 10^6$$

where, A is the permeation area of samples, and W_i and W_f are the initial and final weight of bottles, respectively. The experiment was conducted at 35°C as the end application of the hydrogel on human skin, which has a temperature of 37.2°C [26].

ATR-FTIR Analysis

In order to analyze MC/PVP hydrogel and MC/PVP/ZnO nanocomposites, ATR-FTIR spectroscopy had been used. A Perkin Elmer FTIR spectrophotometer (Model: Paragon 500, PerkinElmer, UK) with a sophisticated orbit Attenuated Total Reflectance (ATR) accessory was employed to record the spectra in the 4000-400 cm^{-1} region. The diamond crystal is mounted on the ATR. ATR-FTIR spectrum measurements were made in transmittance mode [27].

UV-Visible Spectroscopy

UV-Vis spectroscopy is an analytical procedure that measures the number of discrete wavelengths of UV or visible light that a sample absorbs or lets through to a reference or blank sample. Spectroscopy is since when chemical compounds take in ultraviolet or visible light; they make different spectra. For the UV-Vis test, a suspension of 1 mL of ZnO NPs was made and sonicated at 6000 rpm for 10 minutes. From 200 to 800 nm, the UV-Vis spectra were taken. UV-visible spectroscopy was also employed to evaluate the DPPH free radical scavenging activity [28].

Dynamic Light Scattering Analysis (DLS)

The particle size distribution of biosynthesized ZnO NPs was achieved by dispersing 10 mg of ZnO NPs in 100 ml of distilled water and sonication for 30 min then tested via (NICOMP 380 ZLS, Dynamic light scattering (DLS) apparatus (PSS, Santa Barbara, CA, USA) [29].

Hydrogel Porosity

Hydrogel porosity (%) was calculated using the following equation:

$$Porosity, \% = \frac{W_w - W_d}{D_w A \delta} \times 100$$

Where Ww is the weight of the wet sample, W_d is the dry sample weight (g), D_w is the density of pure water (g/cm^3), A is the area of membrane in the wet state (cm^2), and δ is the thickness of membrane in the wet state (cm) [30].

Field Emission Scanning Electron Microscopy (FESEM)

The surface morphology of the prepared samples was studied by FESEM images. To investigate the dispersion of nanoparticles within the polymeric matrix, field emission scanning electron microscopy (FESEM) was used with an EDX detector at an accelerating voltage of 5 kV.

Energy Dispersive X-ray Measurement (EDX)

The elemental composition of materials can be determined using the X-ray technique referred to as dispersive X-ray analysis (EDX), which is attached to SEM or TEM instruments. The information produced by EDX analysis consists of spectra with peaks corresponding to the constituent elements of the material understudy and is additionally feasible for image analysis and elemental mapping of the sample [31].

Assay of Antibacterial Activity

The resulting films were then cut into a 3 mm diameter disk. The films were placed on the culture surface of Escherichia coli and Staphylococcus aureus bacteria on the agar medium. After 24 hours of incubation at 37°C, the zones of inhibition around the disc were measured in millimeters [32].

Antioxidant Activity Test

The 2,2-diphenyl-1-picrylhydrazyl radical was used to test the antioxidant activity of bio-nanocomposite films. At 517 nm, the samples' absorbances were measured.

$$Free\ Radical\ Scavenging\ Activity,\ \% = \frac{(A_c - A_s)}{A_c} \times 100$$

where A_c and A_s were the absorbances of DPPH of the control and test film, respectively [33].

Cytotoxicity by Hemolytic Potentiality Test

The prepared bio-nanocomposites were tested for hemolytic activity using fresh sheep blood with saline adding trisodium citrate as a blood anticoagulant, incubated at 37°C, taken distilled water for 100% hemolysis, and saline solution for 0% hemolysis. The absorbance of the supernatant at 545 nm was measured, and the hemolysis was estimated as follows:

$$Hemolysis,\ \% = \frac{OD_{sam} - OD_{neg}}{OD_{pos} - OD_{neg}} \times 100$$

Where OD_{sam}, OD_{neg} and OD_{pos} are the adsorptions of the sample, negative control, and positive control, respectively [34].

Biodegradation Study

The dried samples with 4×4 cm^2 dimensions were weighed to determine their initial weight (Wi) before being immersed in deionized water for 24 hours. Natural degradation of the samples was observed for 4 weeks, following which samples were taken from the soil, cleaned to remove mud from the surface, and dried at 80°C for 8 hours.

$$Rate\ of\ Bio\deg radation, R_B = \frac{W_i - W_d}{W_i} \times 100$$

Where W_d is the dried weight of the hydrogel. W_i is the initial weight of the hydrogel; RB is the rate of biodegradation of the sample [35].

Results and Discussion

Gel Content

Gel content is an important characteristic since it controls the amount of cross-linking that occurs in the hydrogel network. A sol-gel conversion of a finite crosslinked polymer into an infinite number of molecules results in a hydrogel. The portion of the hydrogel that is left over after the sol has been removed is referred to as the gel content, and a higher gel content % indicates a stiffer hydrogel. The gel content of the prepared MC/PVP hydrogel was 76% and it decreased to 70% gradually with the addition of 2, 4, and 6% ZnO NPs to the polymer matrix.

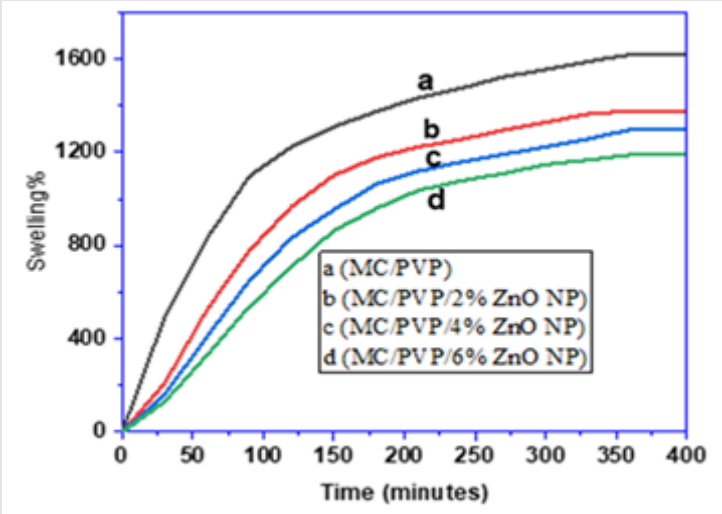

Figure 2: Swelling, % vs time of the prepared samples.

Swelling Behavior

The ability to absorb fluids (blood plasma or serum) from wounds is one of the primary properties of hydrogel wound dressings. The swelling behaviour of the hydrogels was evaluated using distilled water rather than blood (because blood plasma contains around 90-92% water), and at room temperature, the dried hydrogel sample was allowed to expand in distilled water. As depicted in Figure 2, there was a fast swelling for the first 100 minutes, followed by a slower continuous swelling for 270-360 minutes (for equilibrium swelling). For MC/PVP without ZnO NPs, the maximum swelling degree reached was 1610%, and it tended to decrease as the proportion of ZnO NPs in the polymer matrix increased, as depicted in Figures 2a-2d. Since the ZnO NPs occupy the pores of the gel, there is less space for water to attach to the polymeric framework.

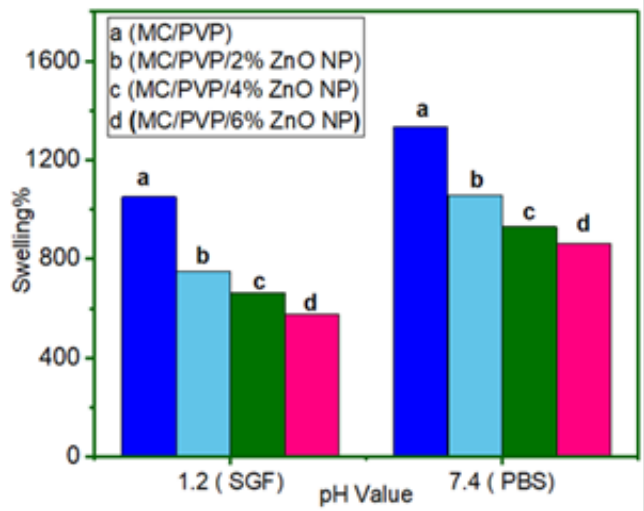

Figure 3: Swelling, % vs pH value of the prepared samples.

As shown in Figure 3 the water uptake behaviour of the films was tested in two solutions with pH values of 7.4 (Phosphate Buffer Saline, PBS) and 1.2 (Stimulated Gastric Fluid, SGF) to test the pH sensitivity of hydrogels. All samples absorbed more water when the pH was higher, such as 7.4. The electrostatic repulsive forces between negatively charged sites (COO-) result in an increase in the water absorption capacity when the pH is higher than the pKa of carboxylic groups (pKa 4-5) [36]. Low pH values cause most carboxylate anions to protonate. Lower levels of water absorption occur when the electrostatic repulsion between carboxylate groups is reduced. Additionally, the fact that there are more hydrogen bonding connections between carboxylate groups, which implies a larger physical crosslinking, may be the cause of the hydrogel films' lower capacity to absorb water [37].

Water Vapour Transmission Rate Test

High WVTR results in the development of scars, while low WVTR leads to the formation of exudates and enhanced bacterial growth. The WVTR values for MC/PVP, MC/PVP with 2, 4, and 6% ZnO NPs incorporated hydrogel films were 2450, 2345, 2286, and 2215 g/m^2-day, respectively. To prevent the wound from drying out and losing water, as well as the development of exudates in the wound bed, the ideal wound dressing should have a WVTR of 2,000-2,500g/m^2-day. Thus, our synthesized nanocomposites are best suited for use as wound dressings.

ATR-FTIR Analysis

FTIR spectra of pure MC, PVP, MA, biogenic ZnO NPs, and MC/PVP hydrogels with and without ZnO NPs addition were shown in Figure 4. Peaks in the 3300 cm^{-1} - 3500 cm^{-1} wave number range for all samples reveal the existence of hydroxyl groups (-OH), which imply hydrophilic properties and the ability of the hydrogel to absorb water, and the peaks in the 2800-3000 cm^{-1} wave number range for all samples indicate C-H stretching vibrations. The absorption peaks that appeared at 1430 cm^{-1} showed the presence of lignin C=O stretching and more intense vibrations at 1060 cm^{-1} indicate the presence of ether (C–O-C), 1430 cm^{-1} for –CH2- wagging in MC. PVP spectra could be stated as 1,640 cm^{-1} for C = O vibration. 1281 cm^{-1} for C–N stretching vibration, and maleic acid 1704 cm^{-1} for C=O stretching. Hydrogel without ZnO NPs showed a new peak at 1741 cm^{-1} indicating an esteric group & hydrogel with ZnO NPs shows also esteric bond at 1745 cm^{-1} and a new peak for the presence of ZnO NPs particles at 432 cm^{-1}. As a consequence, it could be concluded that the chemical process of crosslinking between MC and maleic acid had been executed successfully.

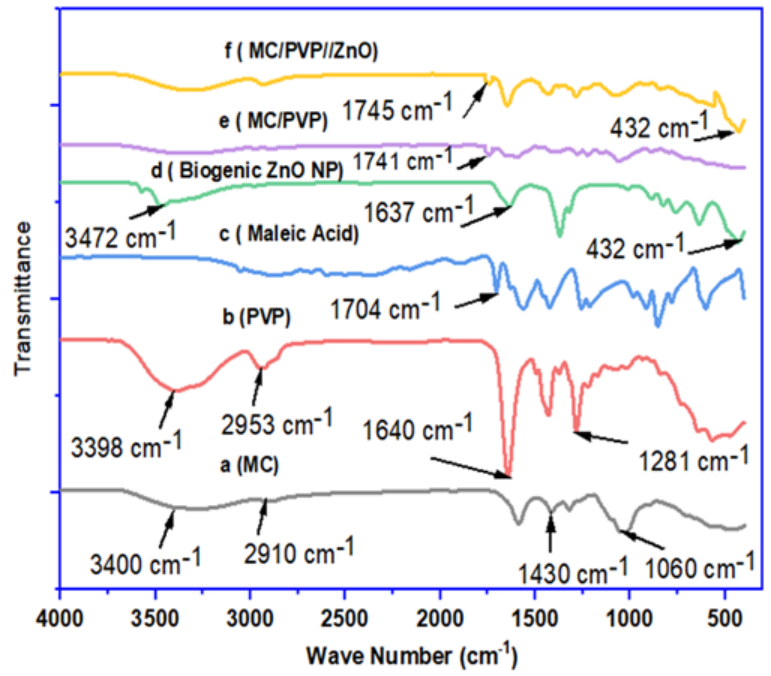

Figure 4: FTIR Spectra of the different samples.

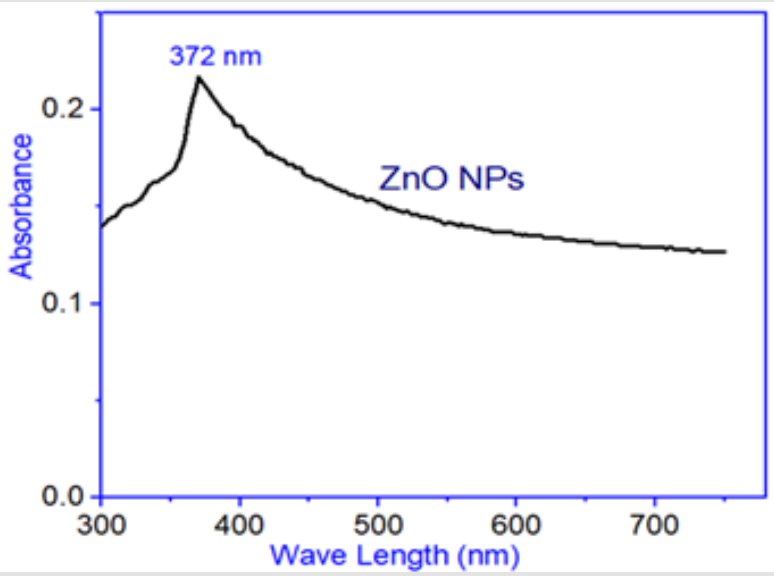

Figure 5: The UV–Visible spectrum of the bio-synthesized ZnO-NPs using Azadirachta indica.

UV-Visible Spectroscopic Analysis

As illustrated in Figure 5, UV-Visible spectroscopy was used to investigate the optical characteristics of neem leaf extract-assisted ZnO NPs. The absorbance peak at 372 nm demonstrates that biosynthesis was used to produce ZnO NPs. This is due to the intrinsic band gap absorption of ZnO, caused by electron transitions from the valence band to the conduction band (O2p–Zn3d). The evaluated value is less than that of bulk ZnO, which is 380 nm, and there is a blue shift in excitonic absorption, indicating that bulk metal oxides have a large band gap and less ability to interact. When their sizes are decreased, however, they become more responsive, and their ability to interact can be deduced from how well they reflect and absorb light.

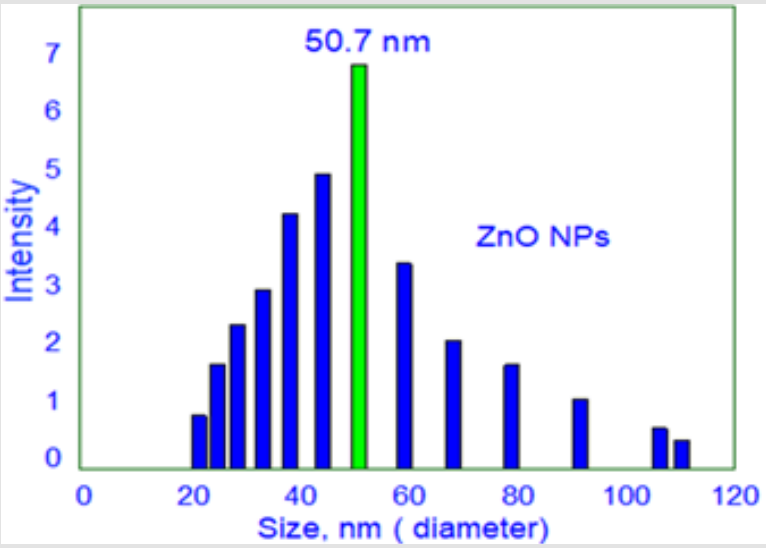

Figure 6: The DLS analysis of the bio-synthesized ZnO-NPs.

Dynamic Light Scattering Analysis (DLS)

DLS is a new method that is widely used to estimate the hydrodynamic diameter of nanoparticle suspensions based on the Brownian motions of the particles. For the measurement, ZnO NPs in water were used. Figure 6 shows that the ZnO NPs that were made are stable. From the histogram study, particles with a 50.7 nm diameter made the most of the particles' volume.

Hydrogel Porosity

The pore structure of the nanocomposite hydrogel was evaluated. When ZnO NPs content is 0 wt%, sparse pores can be observed and the porosity is 88%, With increasing of ZnO NPs to 2 to 6%, the porosity decreases to 80%. The dressings' high porosity helps to absorb more exudate from a wound surface and prevent wound infection caused by exudates.

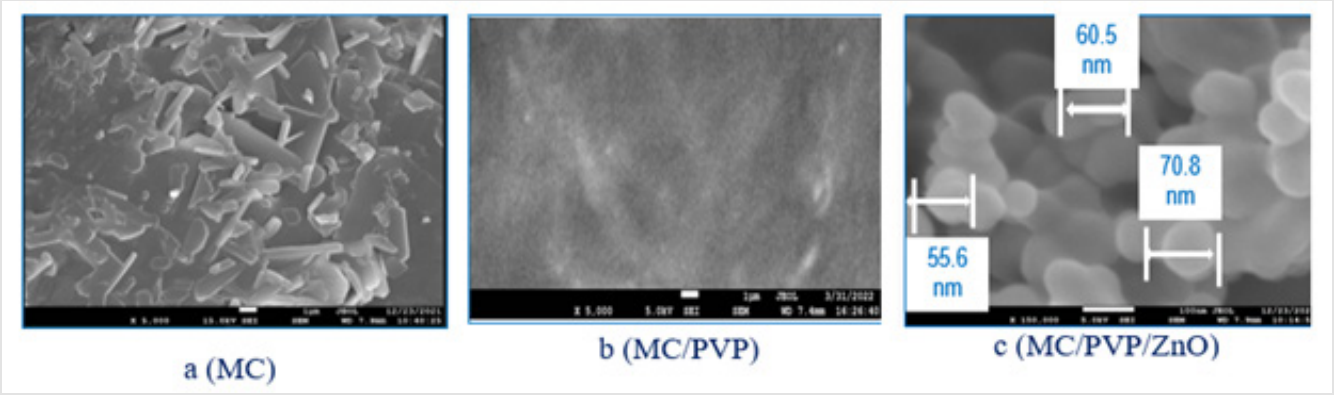

Figure 7: FESEM images of

a) MC,

b) MC/PVP, and

c) MC/PVP/ZnO bio-nanocomposites.

Field Emission Scanning Electron Microscopy

In Figures 7a-7c, as FESEM images, MC show the crystalline and fibre type morphology, while hydrogel without ZnO NPs showed a homogeneous blended structure and confirms crosslinking among MC, PVP and maleic acid successfully. FESEM images of the cross-section of the MC/PVP/ZnO composite film revealed that there were no voids in the nanocomposite indicating that the fillers are compatible with the polymer matrix and intermolecular binding. It assured the presence of ZnO NPs in the hydrogel with hydrophobic interaction. Energy-dispersive X-ray Analysis (EDX). The EDX analyses and the elemental composition of prepared hydrogels with ZnO NPs in both mass and atom% are listed in the following Table 1. The presence of N and Zn atoms indicates the existence of PVP & ZnO NPs in the prepared bio-nanocomposites.

Table 1: EDX of MC/PVP/ZnO nanocomposite hydrogel.

Sample	Elements	Mass, %	Atom, %
MC/PVP/ZnO	C	45.35	53.4
	N	9.06	9.11
	O	40.41	35.59
	Zn	5.18	1.9

Antibacterial Activity of the Prepared Composites

The antimicrobial activities of the MC/PVP, MC/PVP/ZnO (2, 4 and 6%), and antibiotic (control) are determined by testing them against Escherichia coli and Staphylococcus aureus bacteria. The results from Table 2 showed that prepared hydrogels are more effective against *E. coli* than *S. aureus* bacteria and the zone of inhibition increases with the increase of ZnO NPs% in the hydrogel structures. That is to say, ZnO NPs have strong antibacterial activity.

Table 2: Zone of Inhibition of prepared hydrogels.

Hydrogel Samples	Zone of Inhibition (mm)	
	S. aureus	*E. coli*
MC/PVP	0.45	0.65
MC/PVP/ ZnO (2%)	1.4	2.0
MC/PVP/ZnO (4%)	3.2	4.0
MC/PVP/6% ZnO (6%)	5.2	5.75
Amoxycillin (250 mg)	10.2	12.4

Antioxidant Test of the Prepared Composites

The results from Table 3 showed that the DPPH free radical scavenging activity of composites rises with the increasing conc. of ZnO NPs (0.2 mg/ml—35 %; 0.4 mg/ml-40.5 %; 0.6 mg/ml-46.2 %) in the polymer matrix and these results are close to the DPPH RSA% of ascorbic acid.

Table 3: DPPH free radical scavenging activity of the MC/PVP/ZnO nanocomposites and ascorbic acid.

Conc. of the Antioxidant	DPPH RSA, %	
	ZnO NPs	Ascorbic acid
0.2 $mgml^{-1}$	35	45
0.4 $mgml^{-1}$	40.5	50.5
0.6 $mgml^{-1}$	46.2	60.4

Effect of ZnO NPs on Blood Compatability

The hemolytic activity of MC/PVP and 2, 4, and 6% ZnO NPs incorporated bio-composites were calculated as 1.2, 1.75, 2.25 and 2.82% which showed negligible hemolytic properties according to the American Society for Testing and Materials. So, the prepared bio-nanocomposites were considered nonhemolytic materials.

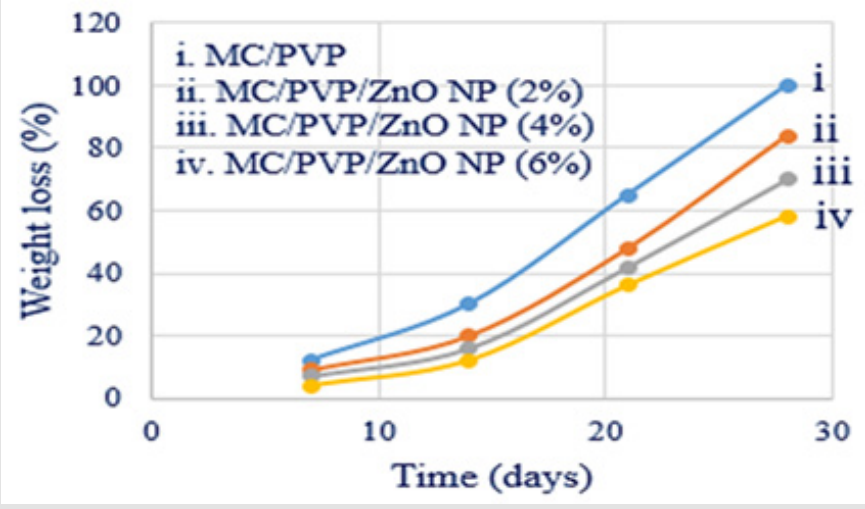

Figure 8: Biodegradation rate of the prepared nanocomposites.

Biodegradability Test of the Prepared Composites

In Figure 8, the MC/PVP film was disintegrated 100% in 28 days but for 2, 4, and 6% ZnO NPs incorporated nanocomposites after 28 days, the weight loss% was 84, 72, and 58%. So, the prepared hydrogels are moderately biodegradable.

Conclusion

The ZnO-loaded MC/PVP nanocomposite hydrogels were successfully prepared by the solution casting method. FTIR, FESEM and EDX results supported the presence of ZnO nanoparticles in prepared bio-nanocomposites. The swelling ratio was maximum for MC/PVP gels, but it decreased with increasing of ZnO NPs. It demonstrated antibacterial activity against *E. coli* and *S. aureus* bacteria and more ZnO NPs loaded composites scavenged more DPPH free radicals. Based on the results, all samples are biodegradable, non-toxic, water vapour permeable, and porous. So, the novel MC/PVP/ZnO bio-nanocomposites would be a better alternative to the traditional wound dressing.

References

1. Gupta B, Agarwal R, Alam MS (2011) 9 - Hydrogels for wound healing applications. In: Biomedical hydrogels – Biochemistry, manufacture and medical application. In: Rimmer S (Edt.)., Woodhead Publishing, pp. 184-227.
2. Chai Q, Jiao Y, Yu X (2017) Hydrogels for Biomedical Applications: Their Characteristics and the Mechanisms behind Them. Gels 3(1): 6.
3. Kołodyńska D, Skiba A, Górecka B, Hubicki Z (2016) Chapter 4- Hydrogels from Fundaments to Application. In: Emerging Concepts in Analysis and Applications of Hydrogels. In: Majee SB (Edt.)., IntechOpen, pp. 71-100.
4. Chai Q, Jiao Y, Yu X (2017) Hydrogels for Biomedical Applications: Their Characteristics and the Mechanisms behind Them. Gels 3(1): 6.
5. Li L, Wang Y, Pan L, Shi Y, Cheng W, et al. (2015) A Nanostructured Conductive Hydrogels-Based Biosensor Platform for Human Metabolite Detection. Nano Letters 15(2): 1146-1151.
6. Kim MH, Park H, Nam HC, Park SR, Jung JY, et al. (2018) Injectable methylcellulose hydrogel containing silver oxide nanoparticles for burn wound healing. Carbohydrate Polymers 181: 579-586.
7. Teodorescu M, Bercea M, Morariu S (2018) Biomaterials of PVA and PVP in medical and pharmaceutical applications: Perspectives and challenges. Biotechnology Advances 37(1): 109-131.
8. Higa OZ, Rogero SO, Machado LDB, Mathor MB, Lugão AB (1999) Biocompatibility study for PVP wound dressing obtained in different conditions. Radiation Physics and Chemistry 55(5-6): 705-707.
9. Seki Y, Altinisik A, Demircioğlu B, Tetik C (2014) Carboxymethylcellulose (CMC)–hydroxyethylcellulose (HEC) based hydrogels: synthesis and characterization. Cellulose 21(3): 1689-1698.
10. Wang M, Xu L, Hu H, Zhai M, Peng J, et al. (2007) Radiation synthesis of PVP/CMC hydrogels as wound dressing. Nuclear Instruments and Methods in Physics Research Section B: Beam Interactions with Materials and Atoms 265(1): 385-389.
11. Saha N, Saarai A, Roy N, Kitano T, Saha P (2011) Polymeric Biomaterial Based Hydrogels for Biomedical Applications. Journal of Biomaterials and Nanobiotechnology 2(1): 85-90.
12. Ji T, Zhang R, Dong X, Sameen DE, Ahmed S, et al. (2020) Effects of Ultrasonication Time on the Properties of Polyvinyl Alcohol/Sodium Carboxymethyl Cellulose/Nano-ZnO/Multilayer Graphene Nanoplatelet Composite Films. Nanomaterials 10(9): 1797.
13. Abou-Yousef H, Kamel S (2015) High efficiency antimicrobial cellulose-based nanocomposite hydrogels. Journal of Applied Polymer Science 132(31): 42327.
14. Yu J, Cheng L, Jia Z, Han X, Xu H, et al. (2022) Injectable Methylcellulose and Hyaluronic Acid Hydrogel Containing Silver Nanoparticles for Their Effective Anti-microbial and Wound Healing Activity After Fracture Surgery. Journal of Polymers and the Environment 30: 1330-1343.
15. Safawo T, Sandeep B, Pola S, Tadesse A (2018) Synthesis and characterization of zinc oxide nanoparticles using tuber extract of anchote (*Coccinia abyssinica* (Lam.) Cong.) for antimicrobial and antioxidant activity assessment. Open Nano 3: 56-63.
16. Yadollahi M, Gholamali I, Namazi H, Aghazadeh M (2015) Synthesis and characterization of antibacterial carboxymethyl cellulose/ZnO nanocomposite hydrogels. International journal of biological macromolecules 74: 136-141.
17. Cotton GC, Lagesse NR, Parke L, Meledandri CJ (2019) Antibacterial Nanoparticles. Reference Module in Materials Science and Materials Engineering. In: Comprehensive Nanoscience and Nanotechnology 3. In: Andrews DL, Lipson RH, Nann T (Eds.)., Elsevier.
18. Husain MSB, Gupta A, Alashwal BY, Sharma S (2018) Synthesis of PVA/PVP based hydrogel for biomedical applications: a review. Energy Sources, Part A: Recovery, Utilization, and Environmental Effects 40(20): 1-6.
19. Kumar PTS, Lakshmanan VK, Anilkumar TV, Ramya C, Reshmi P, et al. (2012) Flexible and Microporous Chitosan Hydrogel/Nano ZnO Composite Bandages for Wound Dressing: *In Vitro* and *In Vivo* Evaluation. ACS Applied Materials & Interfaces 4(5): 2618-2629.
20. Ramamoorthy S, Surendhiran S, Kumar DS, Murugesan G, Kalaiselvi M, et al. (2022) Evaluation of photocatalytic and corrosion properties of green synthesized zinc oxide nanoparticles. Journal of Materials Science: Materials in Electronics 33(12): 9722-9731.
21. Handago DT, Zereffa EA, Gonfa BA (2019) Effects of Azadirachta indica leaf extract, capping agents, on the synthesis of pure and Cu doped ZnO-nanoparticles: a green approach and microbial activity. Open Chemistry 17(1): 246-253.
22. Hossain M, Afroz S, Islam MU, Alam AKMM, Khan RA, et al. (2021) Synthesis and characterization of polyvinyl alcohol/water-hyacinth (*Eichhornia crassipes*) based hydrogel by applying gamma radiation. Journal of Polymer Research 28(5): 167.
23. Segiet D, Jerusalem R, Katzenberg F, Tiller J (2020) Investigation of the swelling behavior of hydrogels derived from high-molecular-weight poly(2-ethyl-2-oxazoline). Journal of Polymer Science 58(5): 747-755.
24. Seki Y, Altinisik A, Demircioğlu B, Tetik C (2014) Carboxymethylcellulose (CMC)-hydroxyethylcellulose (HEC) based hydrogels: synthesis and characterization. Cellulose 21(3): 1689-1698.
25. Khorasani MT, Joorabloo A, Moghaddam A, Shamsi H, Moghadam ZM (2018) Incorporation of ZnO nanoparticles into heparinised polyvinyl alcohol/chitosan hydrogels for wound dressing application. International Journal of Biological Macromolecules 114: 1203-1215.
26. Hossain M, Afroz S, Islam MU, Alam AKMM, Khan RA, et al. (2021) Synthesis and characterization of polyvinyl alcohol/water-hyacinth (*Eichhornia crassipes*) based hydrogel by applying gamma radiation. Journal of Polymer Research 28(5): 167.

27. Fakhari S, Jamzad M, Fard HK (2019) Green synthesis of zinc oxide nanoparticles: a comparison. Green Chemistry Letters and Reviews 12(1): 19-24.

28. El-Sayed HS, El-Sayed SM, Youssef AM (2021) Novel approach for biosynthesizing of zinc oxide nanoparticles using Lactobacillus gasseri and their influence on microbiological, chemical, sensory properties of integrated yogurt. Food Chemistry 365: 130513.

29. Koromilas N, Anastasopoulos C, Oikonomou E, Kallitsis J (2019) Preparation of Porous Polymeric Membranes Based on a Pyridine Containing Aromatic Polyether Sulfone. Polymers 11(1): 59.

30. Gupta BD, Semwal V, Pathak A (2020) Nanotechnology-based fiber-optic chemical and biosensors. Nano-Optics, pp. 163-195.

31. Hosseini SN, Pirsa S, Farzi J (2021) Biodegradable nano composite film based on modified starch-albumin/MgO; antibacterial, antioxidant and structural properties. Polymer Testing 97: 107182.

32. Arrua D, Strumia MC, Nazareno MA (2010) Immobilization of Caffeic Acid on a Polypropylene Film: Synthesis and Antioxidant Properties. Journal of Agricultural and Food Chemistry 58(16): 9228-9234.

33. Lu Z, Gao J, He Q, Wu J, Liang D, et al. (2017) Enhanced antibacterial and wound healing activities of microporous chitosan-Ag/ZnO composite dressing. Carbohydrate Polymers, 156: 460-469.

34. Xu Y, Hanna MA (2005) Preparation and properties of biodegradable foams from starch acetate and poly (tetramethylene adipate-co-terephthalate). Carbohydrate Polymers 59(4): 521-529.

35. Morsi MA, Rajeh A, Menazea AA (2019) Nanosecond laser-irradiation assisted the improvement of structural, optical and thermal properties of polyvinyl pyrrolidone/carboxymethyl cellulose blend filled with gold nanoparticles. Journal of Materials Science: Materials in Electronics 30: 2693-2705.

36. Ramadoss P, Regi T, Rahman MI, Arivuoli D (2020) Low-cost and biodegradable cellulose/PVP/activated carbon composite membrane for brackish water treatment. Journal of Applied Polymer Science 137(22): 48746.

37. Purkait P, Bhattacharyya A, Roy S, Maitra S, Das GC, et al. (2023) Green synthesis of ZnO nanoparticle using Trema orientalis (L) leaf: an efficient photocatalyst for degradation of zoxamide fungicide in aqueous organic media under UV light irradiation. International Journal of Environmental Analytical Chemistry 103(2): 307-325.

ISSN: 2574-1241

DOI: 10.26717/BJSTR.2023.49.007795

Md. Ibrahim H Mondal. Biomed J Sci & Tech Res